JOURNAL OF CATALYSIS 127, 761–776 (1991)

Studies on Chromia/Zirconia Catalysts

II. ESR of Chromium Species

A. CIMINO, D. CORDISCHI, S. DE ROSSI, G. FERRARIS, D. GAZZOLI, V. INDOVINA, M. OCCHIUZZI, AND M. VALIGI

Centro di Studio SACSO CNR c/o Dipartimento di Chimica, Università La Sapienza, 00185 Roma, Italy

Received January 2, 1990; revised June 18, 1990

The characterization of CrO_x/ZrO_2 samples (Cr content 0.05 to 6 wt%) by means of ESR spectroscopy is reported. On samples heated in O_2 at increasing temperatures up to 1173 K, the presence of Cr(V) (γ-signal, $g_\parallel = 1.960$ and $g_\perp = 1.979$) is detected by ESR. Its concentration (Cr(V) ions nm^{-2}) is found to increase with temperature, remaining about constant above 773 K. Experiments with the ^{53}Cr isotope allow assignment of the species to a surface mononuclear chromyl-complex in a square pyramidal configuration. At higher temperatures (generally at $T \geq 973$ K, depending also on textural features of the ZrO_2 support and Cr content) the ESR signals of (i) a chromia-like phase (β'-signal, $g = 1.98$ and $\Delta H_{pp} = 1500$–1800 G) and (ii) α-Cr_2O_3 ($g = 1.98$, $\Delta H_{pp} = 480$–500 G, spectra recorded at $T \geq 308$ K) are observed in addition to Cr(V). The particle size of the β'-species is too small (≤ 7 nm) to show strong antiferromagnetic interactions. On samples reduced with CO, the γ-signal sharply decreases with increasing temperature of the reduction, and disappears at 623 K. In the more concentrated samples and after extensive reduction only, an ESR signal from Cr(III) is observed (δ-species, $g \simeq 2.2$ with a broad maximum at g in the range 3.8 to 5.0), and assigned to weakly interacting Cr(III) ions exposed on the surface of ZrO_2. If reduced samples are treated with H_2O at increasing temperatures up to 1073 K, the selective oxidation of Cr(II) to Cr(III)-β species ($g = 1.98$, $\Delta H_{pp} = 1500$–1600 G) is observed. Species Cr(III)-β and Cr(III)-β' differ from each other by cluster size only, as indicated by their different redox behavior. Reoxidation with O_2 at room temperature only minimally restores the γ-signal, and hardly affects the δ-signal. Full reversibility is achieved upon heating in O_2 at 773 K. ESR results and average oxidation numbers from redox cycles allow the identification of two distinct redox couples on the ZrO_2 surface: Cr(III)/Cr(V) and Cr(II)/Cr(VI). The stabilization effect of the ZrO_2 matrix on the various chromium species is discussed.

INTRODUCTION

Reasons for studying chromia supported on zirconia, and specifically the interest of the system for catalytic reactions such as hydrogenations, are illustrated in Part I, where preparation and characterization of the system by means of chemical, DTA, X-ray, and XPS techniques are reported (*1*). Characterization of the system by means of ESR spectroscopy is given here. Preliminary reports of chromium species detected by ESR have been previously presented when discussing catalytic activity of reduced chromia/zirconia for H_2–D_2 equilibration (*2*), and also in connection with the nature of chromium species identified by means of IR spectroscopy (*3*).

Several examples can be found which show that ESR characterization of catalysts containing transition metal ions (tmi) make a valuable contribution to the understanding of the system. On the other hand, the approach is, in principle, exposed to the criticism that ESR frequently detects only a small fraction of total tmi present in the catalyst. In addition to the more trivial reason of tmi with $S = 0$, the main reasons for this limitation arise from surface heterogeneity and/or unfavorable relaxation features, which render the ESR spectra of some oxidation states of the tmi nondetectable or

0021-9517/91 $3.00

very broad and, therefore, difficult to assign. As regards the specific case of chromium on zirconia, Cr(VI) has $S = 0$ and hence no ESR spectra, and no report exists of Cr(IV) and Cr(II) on surfaces; surface Cr(III) species give broad ESR signals, whereas Cr(III) in solid solution and Cr(V) possess proper features for identification by ESR. The use of ^{53}Cr-enriched samples provides an additional tool for the characterization of the system. With due consideration given to ESR limitations, it is, however, possible to reach a detailed picture of the chromium species present on the surface of zirconia after various treatments. To this end, it is essential to have the background information on the average oxidation state, $\bar{n}$, of chromium by chemical titrations (*1*) on the same samples as those on which ESR spectra are taken. Complementary information from IR and XPS techniques are also of great value (*1*, *3*), especially with respect to the identification of Cr(II) and Cr(VI) species. The spectroscopic features of the ESR signals are presented and rationalized in the Results section, where their assignment is given. A discussion of the different Cr species, in relation to the surface chemistry processes taking place during the various catalyst treatments, is given in the Discussion.

EXPERIMENTAL

Catalysts

The ZrO_2 support and CrO_x/ZrO_2 samples used in the present investigation (Table 1) were portions of those reported in Part I (*1*), where details of preparation and characterization are given. Here it is sufficient to recall that chromium-containing samples are designated as ZC*x*(T), where *x* is the approximate Cr metal content (wt%) and *T* is the temperature (*T*/*K*) at which the starting zirconium oxide was heated before chromium uptake from a CrO_3 solution at pH = 1. Capital letters identify distinct preparations.

In addition to samples mentioned above, ^{53}Cr-enriched specimens (98.6%, ICN Biomedicals Inc.), were prepared at two different chromium contents: ZC0.05(383) and ZCl(383).

TABLE 1

CrO_x/ZrO_2 Samples and Some of Their Features

Sample	Cr content[a] (wt%)	SA[a] ($m^2\ g^{-1}$)
ZC0.05(383)B	0.05	95
ZC0.3(383)B	0.32	115
ZC0.9(383)B	1.03	133
ZC1.7(383)B	2.14	145
ZC5.0(383)B	5.98	160
ZC1.6(673)B	1.60	117
ZC0.25(923)C	0.25	19
ZC0.5(923)B*	0.52	32

[a] Chromium content and surface areas measured after heating in oxygen at 773 K.

Procedure

Experiments were performed in the same circulation apparatus already described (see Part I, redox cycles). In this case, however, the silica reactor was equipped with a side tube for ESR measurements. Samples were generally submitted to standard redox cycles consisting of (i) heating with O_2 at 773 K for 0.5 h (standard oxidation, s.o.) and (ii) subsequent heating with CO at 623 K (standard reduction, s.r.). The effect of other treatments in controlled atmospheres (O_2, air, CO, H_2O) at various temperatures was also investigated. The acquisition or loss of electrons expressed as *e*/Cr (number of electrons)/(total Cr atoms) allowed the variation of the average oxidation number $\bar{n}$ to be followed. The $\bar{n}$ values measured during redox cycles reported in the present paper are in substantial agreement with those reported in Part I (*1*). At the end of each treatment, the powder was transferred to the ESR tube and the spectrum recorded. ESR measurements were generally made at room temperature (RT) or at 77 K on a Varian E-9 spectrometer (generally at X-band

or, in a few cases, at Q-band). In addition, studies of the temperature dependence of the ESR spectra (110 to 520 K) were carried out utilizing the Bruker variable temperature control unit B-ST 100/700. The spectrometer was equipped with an on-line computer for data treatment, which consisted of addition, subtraction, smoothing, baseline drift correction, and integration of ESR spectra (*4*). The computer-simulated spectra were calculated by using the computer program described in Ref. (*5*). Absolute concentration of Cr species contributing to ESR spectra were obtained from the integrated area by using as standard a Varian strong pitch with linear spin density, 3×10^{15} (±20%) spin cm^{-1}.

According to Poole (*6*) the number of spins N_A, is obtained by

$$N_A = N_B(g_B/g_A)^2 \times [S_B(S_B + 1)/S_A(S_A + 1)](\text{area}_A/\text{area}_B),$$

where the subscripts A and B refer to the sample and standard, respectively. Integrated areas were normalized for instrumental factors (modulation and gain). Microwave power, attenuated to avoid saturation effects, was held constant. In all cases, the portion of the ESR tube inside the cavity was filled with the powder, and the linear density of the powder (g cm^{-1}) was determined. From N_A values (spin cm^{-1}), absolute concentrations of a specific chromium species, Cr^{n+}, were calculated as percentage of total Cr weight *or* as a molar fraction of Cr^{n+} ($xCr^{n+} = [Cr^{n+}]/[Cr_{tot}]$) *or* as Cr^{n+} ions nm^{-2}. Surface areas ($m^2\ g^{-1}$) were determined after the various treatments by adsorption of N_2 at 77 K. Due to different features of the various ESR signals (linewidth and temperature dependence), integrations were performed at different temperatures and over different field intervals. Specifically these were at RT over 1 kG for the γ-signal, Cr(V) ($S = \frac{1}{2}$); at RT over 8 kG for Cr(III) species ($S = \frac{3}{2}$), and at 363 K over 8 kG for α-Cr_2O_3 ($S = \frac{3}{2}$). In the latter case, it was more reliable to use as a standard a sample of pure α-Cr_2O_3, previously fired in air at 1273 K.

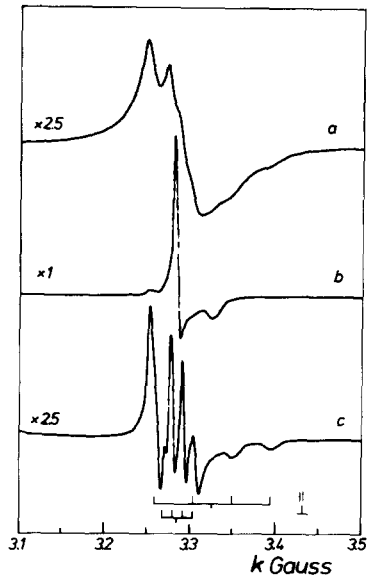

FIG. 1. *ESR spectra of Cr(V) species.* Spectra at RT of CrO_x/ZrO_2 samples heated in O_2 at 773 K. Spectrum a: ^{53}Cr-enriched (98.6%) sample (Cr content 1 wt%); spectrum b: natural isotope (Cr content 0.05 wt%); spectrum c: ^{53}Cr enriched (0.05 wt%).

RESULTS

A. ESR Characterization of Samples in the Oxidized State

1. ESR of Cr(V): γ-Signal

Spectroscopic features of the γ-signal. An intense axial ESR signal ($g_\parallel = 1.960$; $g_\perp = 1.979$) is always detected at RT in all oxidized ZCx(T) samples, after heating in O_2 or in air at various temperatures. A similar signal, observed in other supported CrO_x systems (*7–12*), has been assigned to Cr(V) and designated as the "γ-signal." In more dilute samples, ZC0.05(383), enriched or not with ^{53}Cr (Fig. 1, spectra c and b, respectively), the γ-signal consists of rather narrow lines, and the hyperfine pattern observed on ^{53}Cr-enriched samples ($I = \frac{3}{2}$) shows interaction with *one* chromium nucleus. The same hyperfine pattern is also

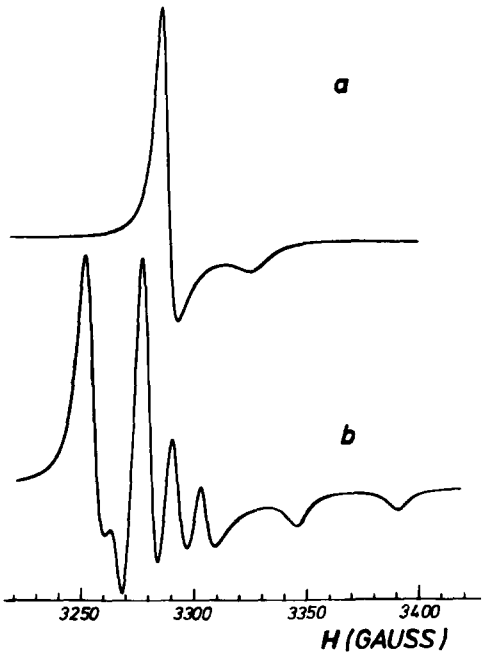

FIG. 2. *Computer-calculated spectra of Cr(V).* Spectrum a: $I = 0$, and spectrum b: $I = \frac{3}{2}$.

observed in more concentrated samples, ZC1(383), even though the spectrum is much less resolved (Fig. 1, spectrum a). In Fig. 2, the spectrum of the γ-signal is compared with that calculated using the g and hf-parameters reported in Table 2. The same parameters are also derived from the analysis of Q-band spectra. In spectra recorded at 77 K, the shape of the signal does not change, and its intensity, evaluated either from the peak height of derivative spectra (h) or from the integrated area (A), increases by a factor of about 3.3; this is in good agreement with the variation expected for a paramagnetic species obeying the Curie law.

Passing now to examine the reactivity and location of the Cr(V) species, it is found that the γ-signal undergoes a reversible broadening in the presence of O_2 at RT. In particular, h-values decrease but A-values remain substantially unchanged in the presence of this gas. For instance, upon addition of O_2 (90 Torr) at RT to the sample ZC0.3(383), a reduction of h by a factor 3 was observed, whereas A remains nearly the same (within 10%). The reversible broadening observed with O_2 shows that the γ-signal is a surface species. The signal remains substantially unchanged both in shape and intensity upon exposure to NH_3 at RT, or to H_2O vapor at RT or higher temperatures up to 723 K. Some changes, albeit small ones, are detected in the spectrum of the ^{53}Cr-enriched samples. In particular, addition of NH_3 at RT and 393 K to the ZC0.05(383) sample leads to a slight decrease of the hf-splitting constants (Table 2).

Assignment of the γ-signal. On the basis of ESR evidence and relying also on the fact that the γ-signal is destroyed by reducing treatments with CO (see below), it is concluded that the species observed on ZC samples after heating in O_2 are mononuclear Cr(V) ions.

As far as the configuration of the species is concerned, the comparison with γ-signals observed in other systems is relevant, and particularly those observed in the CrO_x/SiO_2 system, for which a detailed spectroscopic investigation has been reported by van Reijen and Cossee (*7*). In this system, two distinct γ-signals have been observed after treatment with O_2 at 773 K and assigned to (i) Cr(V) in tetrahedral coordination (CrO_4^{3-} species: the most abundant on SiO_2) and (ii) to Cr(V) in square planar coordination. Besides their different spectroscopic parameters, the two species are also distinguished by their different relaxation times: the first one is detectable only at low temperature ($\leq$20 K), while the other was also observed at RT. Moreover, the low-temperature signal was destroyed by treatments with H_2O, NH_3, or HCl vapors at RT. After these treatments the shape of the ESR spectra became independent of temperature and their intensity followed the Curie law. This behavior was attributed to a change of the Cr(V) coordination from tetrahedral to square pyramidal. It has been suggested (*7*),

TABLE 2

ESR Parameters of γ-Signal and $CrOx_5^{2-}$ Complexes

Species	Treatment[a]	$g_\parallel$	$g_\perp$	$A_\parallel$ (10^4 cm^{-1})	$A_\perp$ (10^4 cm^{-1})	Reference
$Cr(V)/ZrO_2$		1.960	1.979	40.2	11.1	This paper
$Cr(V)/ZrO_2$	+ NH_3 RT	1.960	1.979	39.2	9.2	This paper
$Cr(V)/SiO_2$[b]		1.898	1.975			(*7*)
$Cr(V)/SiO_2$[c]		1.901	1.981			(*10*)
$Cr(V)/SiO_2$	+ NH_3 RT	1.925	1.992	46	19	(*7*)
$Cr(V)/Al_2O_3$		1.920	1.983			(*10*)
$Cr(V)/TiO_2$		1.97[d]				(*12*)
$CrOF_5^{2-}$		1.953	1.969	46	17	(*14*)
$CrOCl_5^{2-}$		2.005	1.976	36	9	(*7*, *14*)

[a] CrO_x/ZrO_2 samples are heated in oxygen at 773 K.
[b] Cr(V) in tetrahedral coordination.
[c] Cr(V) in square pyramidal coordination.
[d] Average value.

however, that the main effect of H_2O vapor is the disappearance of CrO_4^{3-} because of disproportionation of Cr(V) into Cr(VI) and Cr(III).

As regards chromium on the Al_2O_3 support, the spectra of the γ-signal are substantially broader when compared to those of ZC samples, even at very low Cr loadings (0.05 wt%); therefore, detailed information cannot be obtained. Mainly on the basis of the *g*-values and temperature dependence of signal intensity, a square pyramidal configuration has been suggested (*7*). Similarly, Pecherskaya and Kazansky (*10*) have assigned the γ-signal observed on CrO_x/Al_2O_3 samples to square pyramidal chromyl complexes. However, on the basis of reflectance spectra, they concluded that CrO_4^{3-} species were present in addition to square pyramidal complexes.

In contrast with all previous assignments, Spitz (*13*) assigned the γ-signal to trimers of mixed valency ($Cr^{6+} - Cr^{3+} - Cr^{6+}$) with an average oxidation number of 5. The same model has also been postulated by Evans *et al.* (*12*) for the γ-signal observed on the CrO_x/TiO_2 system. The suggestion by Spitz can be rejected in view of the following facts. Experiments with ^{53}Cr-enriched samples demonstrate that the γ-signal observed at RT on SiO_2 (*7*) and on ZrO_2 is due to a mononuclear species. Moreover, the similarity of the *g*-values, conditions of formation and reactivity on the various supports strongly suggest a common assignment. A further argument in favor of the assignment of the γ-species to a surface mononuclear chromyl complex in a square pyramidal configuration comes from the theoretical analysis of *g* and *hf*-parameters carried out for the chromyl complexes $CrOF_5^{2-}$ and $CrOCl_5^{2-}$ (*14*). ESR parameters of these complexes and their relaxation times are, in fact, in good agreement with those of the γ-signal observed on ZrO_2 and other supports (Table 2).

Surface concentration of Cr(V). The surface concentration of Cr(V) (ions nm^{-2}) measured by ESR is reported as a function of temperature of treatment with O_2 or air for various ZC samples, as specified (Fig. 3). In all samples, the Cr(V) concentration increases with temperature up to 773 K. Above this temperature, up to 1173 K, as tested on some samples, the surface concentration of Cr(V) remains constant or slightly

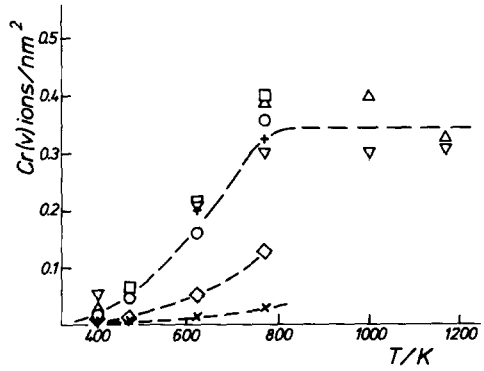

FIG. 3. *Concentration of Cr(V) species (ions nm^{-2}) in CrO_x/ZrO_2 heated in O_2 or in air at various temperatures (T/K).* Samples heated in O_2: (×) ZC0.05(383)B, (◇) ZC0.3(383)B, (○) ZC0.9(383)B, (□) ZC1.7(383)B, (+) ZC5.0(383)B, and (▽) ZC0.25(923)C. Sample heated in air: (△) ZC0.9(383)B.

decreases. As regards the fraction of Cr(V) observed by ESR with respect to the total chromium, this reaches its maximum value at 773 K. At this temperature, the fraction of Cr(V) detected by ESR (γ-signal) monotonically decreases from 50 to 15% with increases in the total chromium concentration from 0.06 to 1.90 ions nm^{-2} (Table 3). The result mainfestly contrasts with the value of the average oxidation number of Cr, $\bar{n} \simeq 5.5$, which indicates that in all ZC samples after s.o., with the exception of the ZC5.0(383)B sample on which some Cr(III) is formed after s.o. (see below), the fraction of Cr(V) is always about 50% (see Part I). The finding that a decreasing fraction of Cr(V) is observed by ESR is, however, intrinsic to this technique, which does not detect magnetically interacting Cr(V) ions (whose concentration increases with Cr content), as reported in the Discussion.

2. *ESR Spectra of Cr(III) Species*

Cr(III) in solid solution of ZrO_2. The ESR spectra of ZCx(383) samples after treatments in oxygen or in air at $T \geq 573$ K show two other signals, in addition to Cr(V) species. The first one, the α-signal with peaks at $g_{eff.} = 5.37$ and 1.40, is present in samples treated at lower temperature ($T \leq 773$ K); the second one, the α′-signal with peaks at $g_{eff.} = 5.80$, 4.45, and 3.25, is predominant at higher temperatures. The spectra consist of sharp peaks typical of species having $S > \frac{1}{2}$ placed in sites of well-defined symmetry (spectra omitted for brevity). The peaks are unaffected by redox treatments, therefore suggesting that they arise from species in solid solution of ZrO_2.

It is found that the variation of the relative intensities of the two signals, α/α', parallels

TABLE 3

Fraction of the Total Chromium Contributing to the γ-Signal ($Cr^{(V)}$) and δ-Signal ($Cr^{(III)}$)

Sample	100 × [Cr(V)]/[Cr_{tot}][a]	100 × [Cr(III)]/[Cr_{tot}][b]	Total chromium (ions nm^{-2})
ZC0.05(383)B	50	[c]	0.06
ZC0.3(383)B	43	[c]	0.32
ZC0.9(383)B	37	13	0.89
ZC1.7(383)B	22	14	1.70
ZC5.0(383)B	7	18	4.30[d]
ZC1.5(673)B	24	10	1.63
ZC0.25(923)C	18	5	1.52
ZC0.5(923)B*	15	9	1.90

[a] CrO_x/ZrO_2 samples heated in O_2 at 773 K (γ-signal).
[b] CrO_x/ZrO_2 samples reduced in CO at 623 K (δ-signal).
[c] Not detectable.
[d] On this sample, after heating in O_2 at 773 K, part of chromium is segregated as Cr(III) (chromia-like species).

that of the tetragonal/monoclinic ratio of the ZrO_2 phase, as determined by X-ray analysis, which shows that the supported chromium opposes the tetragonal to monoclinic transition of ZrO_2 (*1*). In samples of series ZCx(673) and ZCx(923), α and α'-signals are generally absent. Only after treatments at 1173 K is a very weak α'-signal detected (monoclinic zirconia). In samples ZC0.05(383) and ZC1(383), prepared with enriched ^{53}Cr, the peak at $g_{eff.} = 5.37$ (H = 1210 G at X band) splits into four equivalent lines, with hyperfine splitting of 18 G. The ESR analysis, along with X-ray data of the ZrO_2 phases, allows assigning α and α'-signals to isolated Cr(III) ions in solid solution in the tetragonal and monoclinic phases of ZrO_2, respectively. Using the diagrams reported by van Reijen (*15*) for d^3 ions, E/D and $h\nu/D$ ratios (D and E being zero field terms) can be calculated from $g_{eff.}$ values. However, due to the limited number of detectable peaks, only an upper limit of the $h\nu/D$ ratio can be calculated for α and α'-signals. The results give, for the α-signal, $E/D = 0.33$ and $h\nu/D \leq 0.3$ (i.e., $D \geq 1$ cm^{-1}); for the α'-signal, $E/D = 0.10$ and $h\nu/D \leq 0.3$.

An assessment of the fraction of Cr which enters into solid solution in ZrO_2 is rather difficult since the two signals are highly anisotropic, weak, and found together with more intense signals from the other chromium species (Cr(V) at all temperatures and Cr(III)-β' above 973 K). A rough estimate can be obtained by evaluating the contribution of the α (or α') signal to the total integrated area, and an upper value of 5% is calculated. It is concluded that Cr(III) ions do not enter into solid solution in ZrO_2 in samples of series ZCx(673) and ZCx(923), and enter to a very limited extent in samples of series ZCx(383).

Clustered Cr(III) ions on the surface of ZrO_2. Upon heating at rather high temperature (generally at $T \geq 973$ K) in O_2, H_2O, vacuum, or air, the appearance of broad-bands arising from clustered Cr(III) species is detected in more concentrated ZC samples (Cr content ≥ 0.9 ions/nm^{-2}). Two types of such bands have been observed. The first one designated as the β'-signal is a broad and symmetrical line with $g = 1.98$ and $\Delta H_{pp} = 1500$–1800 G (Fig. 4, spectrum a). Its shape and linewidth change somewhat at 77 K and its intensity (A) does not follow the Curie law. The conditions which lead to the formation of the β'-species (atmosphere and temperature) are reported in Table 4 for three representative samples. It can be seen that the species is formed at lower temperature on ZCx(383) samples when compared to ZCx(923) samples. The presence of the β'-signal in the most concentrated sample, ZC5.0(383), even after heating at 773 K accounts for the lower $\bar{n}$ value (4.8) found on this sample in comparison to all other ZCx(T) samples. The second band is a symmetrical line of Lorentzian shape ($g = 1.98$ and $\Delta H_{pp} = 480$ to 500 G) detectable on spectra recorded at $T \geq 308$ K only, disappearing abruptly below this tempera-

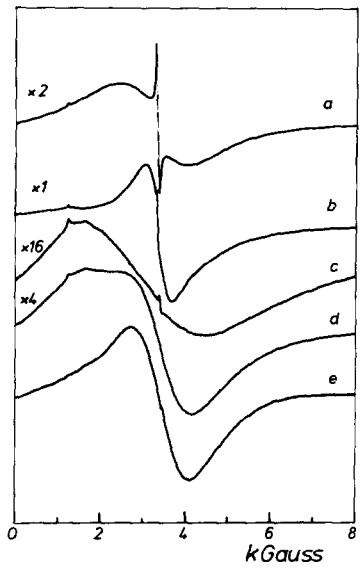

FIG. 4. *ESR spectra of Cr(III) species.* All spectra on the sample ZC5.0(383)B. Sample heated in O_2 at 973 K: spectra recorded at RT (spectrum a) and at 473 K (spectrum b). Sample first heated in O_2 at 773 K and then reduced with CO at 623 K (spectrum c, recorded at RT). Sample as above after subsequent reaction with H_2O at 773 K (spectrum d, at RT). Spectrum e is the spectrum difference, spectrum d minus spectrum c.

TABLE 4

Segregation of α-Cr_2O_3 on CrO_x/ZrO_2

Sample	Atmosphere	Temperature of the treatment					
		773 K		973 K		1173 K	
		β'^a	α-Cr_2O_3	β'^a	α-Cr_2O_3	β'^a	α-Cr_2O_3
ZC0.9(383)B	Air	−	−	+	−	+	+
	O_2	−	−	+	−	+	−
	H_2O	−	−	++	+	+	++
ZC5.0(383)B	Air	+	−	+++	++	++	+++
	O_2	+	−	+++	+	++	+++
	H_2O	++	−	+++	++	++	+++
ZC0.25(923)C	Air	−	−	−	−	++	−
	O_2	−	−	−	−	+	−

Note. (−) Absent, (+) weak, (++) medium, (+++) strong.
[a] Chromia-like particles of small size (≤7 nm).

ture (Fig. 4, spectrum b) and hence showing the typical behavior of ESR spectra from α-Cr_2O_3 (Néel temperature = 308 K). The signal is therefore assigned to α-Cr_2O_3 segregated on the surface of ZrO_2.

The behavior of the ESR signal arising from α-Cr_2O_3 (specifically, its disappearance in spectra taken at $T < 308$ K) allows the β'-signal to be detected even when an elevated content of α-Cr_2O_3 is present. In Fig. 5, the intensity of integrated spectra (A/a.u.) is reported as a function of the temperature at which the ESR spectra were taken on the ZC5.0(383) sample heated in air at 973 or 1173 K. At $T \simeq 308$ K, a step is clearly seen whose amplitude is proportional to the amount of α-Cr_2O_3 present in the sample. Conditions of formation and intensity of the signal from α-Cr_2O_3 are reported in Table 4, together with those relative to the β'-signal, as already mentioned.

The assignment of the β'-signal is less straightforward. However, (i) the spectroscopic features (in particular g-values, linewidth, lineshape, and variation of intensity with recording temperature), (ii) its formation at high T (Table 4), and (iii) its limited sensitivity to reducing treatments with CO, suggest clustered Cr(III) ions. The size of the Cr(III) cluster is too small to allow for collective interactions, given the long-range antiferromagnetic order existing in α-Cr_2O_3. The behavior of the β'-signal is similar to that found for ESR signals detected on high surface area Cr_2O_3 samples, prepared by the decomposition of chromium hydroxide at low temperature (573 K) (*16*). In these high surface area samples, when the recording temperature is lowered, the

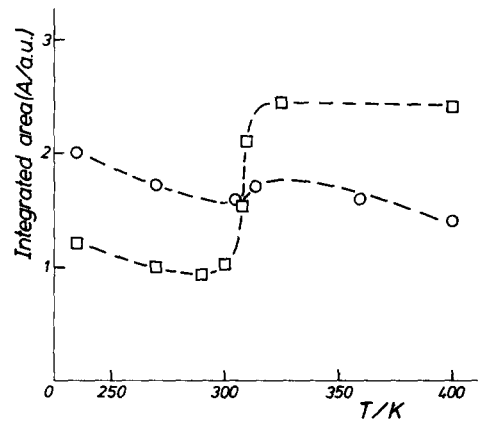

FIG. 5. *The formation of α-Cr_2O_3 in samples heated in O_2 at high temperature.* Normalized integrated area vs recording temperature (T/K). Sample ZC5.0(383)B heated in O_2 at 973 K (○), and 1173 K (□).

ESR signal becomes progressively broader disappearing at about 280 K, a temperature which is substantially lower than the Néel temperature of well-crystallized α-Cr_2O_3 (308 K). An average particle size of 7 nm can be calculated for this high surface area chromia (168 $m^2\ g^{-1}$, from Ref. (*16*)). It is therefore concluded that the cluster size of the Cr(III)-β' species is smaller than 7 nm.

Identification of the oxidized chromium species which leads to the formation of the Cr(III)-β' species and α-Cr_2O_3, when ZC samples are heated in O_2, H_2O, vacuum, or air above 973 K, is now possible. The precursor of the Cr(III)-β' species cannot be Cr(V) ions, since the surface concentration of Cr(V) is found to remain nearly constant upon heating ZC samples in O_2 or in air (Fig. 3) in the same temperature region in which content of the Cr(III)-β' species and α-Cr_2O_3 is found to increase substantially. It is therefore concluded that the Cr (III)-β' species and α-Cr_2O_3 arise from reduction and subsequent clustering of Cr(VI) species, also present in ZC samples heated in O_2 at 773 K (chromates and polychromates on IR evidence (*3*)).

B. ESR Characterization of Reduced Samples

The formation of Cr(III): The δ-signal. Upon reduction with CO in the temperature range 383 to 773 K, a sharp decrease of the γ-signal is observed on all ZCx(T) samples. Simultaneously, $\bar{n}$ values measured by the amount of CO_2 produced are found to decrease progressively. Lowest $\bar{n}$ values ($\bar{n} \simeq 2.5$) are reached after s.r. at 623 K. No further decrease of $\bar{n}$ is observed upon reduction with CO at higher temperatures, up to 773 K. In more concentrated samples (Cr content ≥ 0.9 ions nm^{-2}) and after extensive reduction only, a Cr(III) species is detected in the ESR spectrum: the δ-signal. The spectrum consists of a very broad absorption ($\Delta H_{pp} = 2500$ to 3000 G) starting from zero field, centered at $g \simeq 2.2$ and showing a broad maximum at g in the range 3.8 to 5.0 (Fig. 4, spectrum c). Spectra recorded at 77 K differ from those at RT in shape, and their intensity ratio ($A_{77K}/A_{RT} = 1.5$) does not obey the Curie law.

After s.r., Cr(II) and Cr(III) are the only species present in all ZC samples as demonstrated by ESR, IR (*3*), XPS, and chemical titrations of Cr(II) with H_2O (*1*). Hence, on the basis of $\bar{n} \simeq 2.5$, the fraction of Cr(III) is 50% of the total chromium. The fraction of Cr(III) contributing to the δ-signal can now be evaluated. The results show that this fraction is definitely smaller (18% at most, depending on total Cr content, Table 3) as compared to that estimated from $\bar{n}$ (about 50% of total chromium). On average, at the same Cr content, the fraction is higher in ZCx(383) samples as compared to ZCx(673) and ZCx(923), as shown in Table 3. The large fraction of Cr(III) ions which does not contribute to the δ-signal, taken together with the absence of the δ-signal in more dilute ZC samples and the need of extensive reduction for its detection in more concentrated samples, indicate that isolated Cr(III) ions on the surface of zirconia do not contribute to the δ-signal. On spectroscopic grounds, the lack of the detection of isolated Cr(III) ions on a surface is expected because of variability in the local symmetry of surface sites, which causes variations of the zero-field terms (D and E) for Cr(III) ions ($S = \frac{3}{2}$). These variations, in fact, cause dispersion of the resonance over a very large field interval, thus broadening the signal beyond detection. Having excluded isolated Cr(III) ions, it is concluded that the δ-signal arises only from exchange-coupled Cr(III) ions for which the combined effect of zero-field, dipolar, and exchange terms are operating, thereby rendering the ESR spectrum more narrow and symmetrical (*17, 18*). The features of the Cr(III)-δ species can be further specified by considering its sensitivity to treatments with O_2 (reversible oxidation to Cr(V), see below) which suggests that these weakly interacting Cr(III) ions (clumped species), as well as isolated Cr(III) ions not seen by ESR, are exposed on the surface of ZrO_2.

C. Selective Oxidation and Reduction

Oxidation of s.r. samples with H_2O. The reaction with H_2O selectively oxidizes Cr(II) to Cr(III) (*1*, *2*), therefore allowing the titration of Cr(II) present in s.r. samples from the H_2 evolved during the reaction with H_2O and the characterization by ESR of the Cr(III) species produced from oxidation of the Cr(II).

The experiments were performed by heating the s.r. samples with H_2O vapor (~20 Torr) at increasing temperatures up to 1073 K in the circulation apparatus. After each H_2O treatment at a given temperature the samples were evacuated at the same temperature, the SA determined and the standard redox cycle (s.o. *plus* s.r.) repeated. At each step ESR spectra were taken.

After reaction of s.r. samples with H_2O, a new signal, in addition to the preexisting δ-signal, is observed in the ESR spectrum: the β-signal. This consists of a broad and symmetrical line centered at $g = 1.98$, with $\Delta H_{pp} = 1500$–1600 G (Fig. 4, spectrum e), namely, the same spectroscopic features as the β′-signal, including the dependence of signal intensity on the temperature at which the ESR spectrum is recorded. Therefore, the β-signal is also assigned to Cr(III)-ions assembled in very small clusters. The main difference between β′-Cr(III) species and β-Cr(III) species is the size of these chromia-like clusters. Specifically, dimensions of clusters are smaller for β-species as compared to those of β′ species, especially when the former species are obtained by reaction with H_2O at lower temperature (≤773 K). This statement is substantiated below in considering the redox behavior of this species. In Fig. 6 the intensities of γ, δ, and β-signals are reported, measured when the ZC5.0(383)B sample is reacted with H_2O at increasing temperatures from 623 to 1073 K. Before each treatment with H_2O, the sample was submitted to s.o. and s.r. treatments, in that order.

A first point emerging from an inspection of the data (Figs. 6a and 6b) is the tight

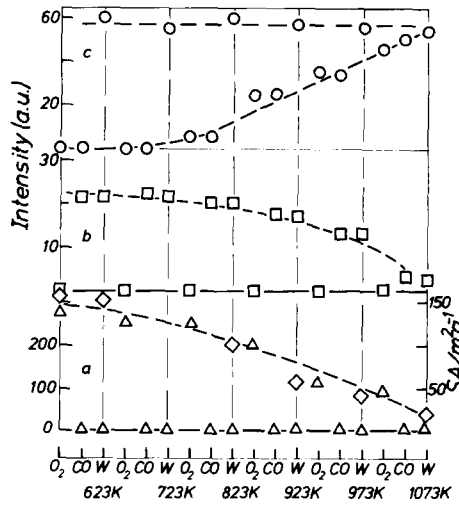

FIG. 6. *The effect of reaction with H_2O on the intensity of Cr(V), Cr(III)-β, and Cr(III)-δ species.* Intensity (a.u.) vs temperature (*T*/*K*) of heating with H_2O. Abscissa lists treatments in sequence. Treatments with O_2 and CO are at 773 K and 623 K, respectively. The temperature of heating with H_2O (W) is as specified. (a) γ-signal (△); (b) δ-signal (□); and (c) β-signal (○). (a) reports also surface areas ($m^2\ g^{-1}$) (◇). Sample ZC5.0(383)B.

relation between Cr(V)-γ and Cr(III)-δ species. In particular, (i) the very similar trend of the two intensity curves, (ii) the detection of Cr(V) after s.o. and its absence after s.r., together with the detection of Cr(III)-δ after s.r. and its absence after s.o., strongly suggest that Cr(III) species reversibly arise from reduction of Cr(V). It is further noted that the intensity decrease of both Cr(V)-γ and Cr(III)-δ signals parallels the decrease of surface area (also reported in Fig. 6a), thus showing that surface concentrations of Cr(V)-γ after s.o. treatments, and that of Cr(III)-δ after s.r., do not depend on the temperature of heating in H_2O vapor up to 1073 K. A second point is the fact that the concentration of Cr(III)-δ is the same *either* after s.r. *or* s.r. plus reaction with H_2O (Fig. 6b and Fig. 4, spectrum d). Coming to the Cr(III)-β species (Fig. 6c), these arise from oxidation with H_2O of the Cr(II) present in s.r. samples. The oxidation leads to Cr(III)-ions in clusters whose size increases with

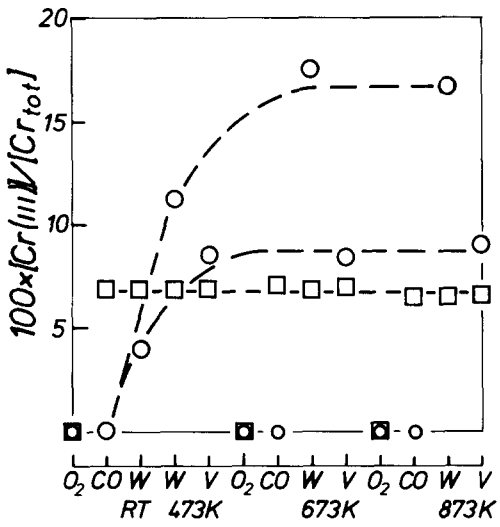

FIG. 7. *Selective oxidation of Cr(II) to Cr(III)-β by reaction with H_2O.* Sample ZC0.5(923)B*. Molar fraction percent of Cr(III)-δ (□) and Cr(III)-β species (○) vs H_2O treatment temperature. Abscissa lists treatments in sequence. Treatments with O_2 and CO are at 773 and 623 K, respectively. Temperatures of heating with H_2O (*w*) and evacuation (*v*) are as specified.

an increase in the temperature of heating in H_2O. The progressive increase of cluster size is supported by the following facts: Cr(III)-β species prepared by reaction with H_2O up to about 923 K can be reversibly reduced to Cr(II) by s.r. treatments, whereas above this temperature the process becomes irreversible (Fig. 6c). At higher temperature (973 K), the ESR signal of well-crystallized α-Cr_2O_3, in addition to that of the β-species, is detected and at 1073 K α-Cr_2O_3 becomes the predominant species. For the sake of clarity, it is explicitly mentioned that β-species obtained after heating s.r. samples with H_2O at $T \geq 923$ K are indistinct from β′-species, both on the basis of spectroscopic features and chemical (redox) behavior.

Another set of selective oxidation experiments with H_2O vapor was carried out on the ZC0.5(923) sample (Fig. 7) at temperatures from RT to 873 K, a temperature range in which the surface area of ZC*x*(923) samples remains nearly constant. After treatment with H_2O at a given temperature, the influence of evacuation at the same temperature has also been examined. In Fig. 7, the molar fraction percent of Cr(III)-β and that of Cr(III)-δ, 100x[Cr(III)]/[Cr_{tot}], is reported after the various treatments. The intensity of the β-signal increases with temperature of the H_2O treatment up to 673 K and remains constant thereafter, thus indicating that at 673 K all Cr(II) is oxidized to Cr(III) (β-species). The intensity of the β-signal is higher (nearly two times) when the sample is not evacuated after the H_2O treatment. This effect is probably due to the lowering of symmetry around Cr(III) ions as a consequence of the elimination of OH groups during evacuation. The intensity of the δ-signal in the s.r. sample is unaffected by H_2O treatment, as observed for the ZC5.0(383) sample (Fig. 6b). Both δ- and β-species are reversibly oxidized by the s.o. treatment ($\bar{n}$ = 5.5). After the latter treatment the γ-signal (not shown in Fig. 7) is restored to its initial intensity. On this sample the formation of well-crystallized α-Cr_2O_3 is not observed at any time.

Controlled oxidation of s.r. samples with O_2. These experiments were carried out in the circulation apparatus in two different ways. In the first one, s.r. samples were exposed to O_2 at RT or 773 K. In the second one, s.r. samples were heated at increasing temperatures from RT to 773 K. In both cases, ESR spectra were taken after each treatment with O_2. Table 5 reports $\bar{n}$ values of (i) s.r. samples (column 2), (ii) samples treated with O_2 at RT (column 3), and (iii) samples treated with O_2 at 773 K (column 4). A full recovery of $\bar{n}$, namely the same values measured after s.o., is observed after treatment with O_2 at 773 K, as already reported in Part I (*1*). At RT, the recovery is partial but rather high, especially in ZC*x*(673) and ZC*x*(923) samples. On the other hand, the ESR signal of Cr(III)-δ shows only a small decrease (15% at most), and the Cr(V) signal only a small increase (25% of the maximum intensity restored) after treatments at RT. The two signals are completely destroyed and reversibly re-

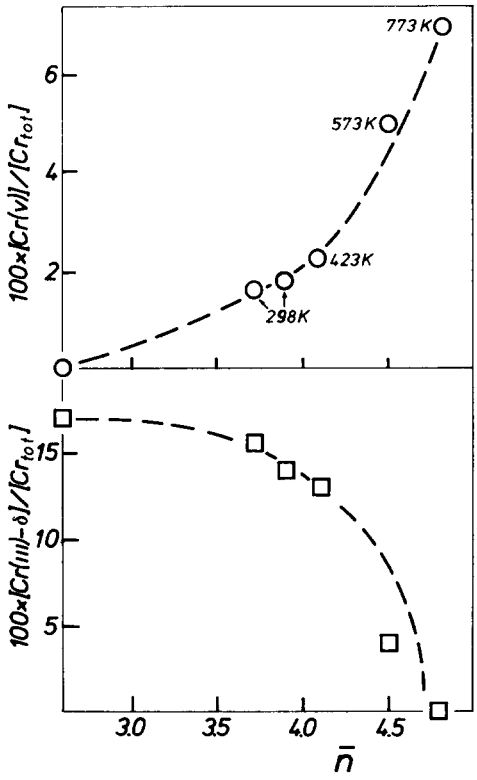

FIG. 8. *Reoxidation of Cr(III)-δ to Cr(V) with O_2 at increasing temperature.* (○) Molar fraction percent of Cr(V) and (□) Cr(III)-δ vs average oxidation number, $\bar{n}$. Oxygen is reacted at increasing temperatures, as indicated, with ZC5.0(383)B previously reduced with CO at 623 K.

stored, respectively, upon heating with O_2 at 773 K. The results show that (i) the prevalent process at RT is the oxidation of Cr(II) to Cr(VI), and (ii) higher temperatures are required for the oxidation of Cr(III) to Cr(V). Both results are confirmed in reoxidation experiments of s.r. samples at in creasing temperatures with O_2. The $\bar{n}$ value is seen to increase from 2.6 to 4.3 before observing a significant increase of the Cr(V)-γ intensity and a decrease of Cr(III)-δ intensity (Fig. 8). Again, the correlation between Cr(V)-γ and Cr(III)-δ species emerges, since their concentration strongly and simultaneously changes at the end of the oxidation process only.

Controlled reduction of s.o. samples. Reduction of ZC0.5(923), ZC1.6(673), and

TABLE 5

O_2 Adsorption on Reduced Samples

Sample	$\bar{n}^a$		
	Before[b] O_2	After[c] O_2 RT	After[d] O_2 773
ZC5.0(383)B	2.6	3.9	4.8
ZC0.9(383)B	2.5	4.2	5.5
ZC1.6(673)B	2.5	4.8	5.5
ZC0.5(923)B*	2.4	4.9	5.6

[a] Average oxidation number of Cr determined as specified in b, c, and d.

[b] Calculated from CO_2 evolved during the reduction with CO at 623 K.

[c] Calculated from O_2 irreversibly adsorbed at RT (not desorbed by evacuation at RT).

[d] Calculated from O_2 adsorbed at 773 K.

ZC5.0(383) samples, after s.o., was performed with CO at increasing temperature in the circulation apparatus. After each treatment with CO, $\bar{n}$-values were determined from CO_2 produced, and ESR spectra were recorded. Results for the sample ZC5.0(923)B* show a monotonic decrease of the concentration of Cr(V) and formation of the Cr(III)-δ species after extensive reduction only, $\bar{n} < 3.2$ (Fig. 9). The latter result is not surprising since isolated Cr(III) species are not seen by ESR, and only weakly interacting clustered Cr(III) species contribute to the δ-signal, as discussed above. The δ-signal, arising from clustered Cr(III) ions, is not observed until an extensive reduction is reached, since exchange and dipolar interactions between clustered ions of different oxidation states (unlike ions) are less effective and tend to broaden the absorption line (*19*). On ZC1.6(673) and ZC0.5(923) samples, the decrease of the Cr(V) concentration with increase of the temperature of reduction is sharper as compared to that observed on ZC5.0(383) sample (Fig. 9). Moreover, on these two samples, the δ-signal is only observed after complete reduction ($\bar{n}$ = 2.5). On all samples, data clearly show that in the early

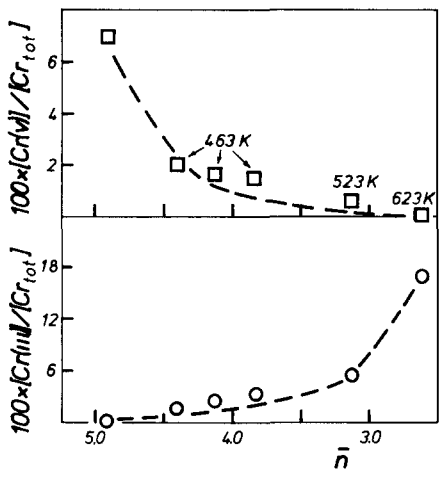

FIG. 9. *Reduction of CrO_x/ZrO_2 with CO at increasing temperature.* (□) Molar fraction percent of Cr(V) and (○) Cr(III)-δ vs average oxidation number, $\bar{n}$. Carbon monoxide is reacted at increasing temperature, as indicated, with ZC5.0(383)B previously heated in O_2 at 773 K.

stages of reduction Cr(V) species, unlike Cr(VI), are preferentially reduced at lower temperatures.

DISCUSSION

The main features of the CrO_x/ZrO_2 system are discussed with the aid of the following scheme, in which the various surface species of chromium have been assembled along with the specification of the treatments required for their formation. Treatments with O_2 and CO are s.o. and s.r., respectively, or at other temperatures, as indicated. It is stressed that all species entered in the scheme have been identified by ESR spectroscopy, with the exception of Cr(VI) and Cr(II), for which the evidence is indirect ($\bar{n}$-values, titration of Cr(II) with H_2O). Direct evidence for Cr(VI) has been given in Part I and for Cr(II) in Ref. (*3*). It is further stressed that in most cases the fraction of total chromium detected by ESR is rather high, generally up to 50% of total chromium, and 80% when α-Cr_2O_3 is segregated after treatments at high temperature. At all stages (1 to 6), the surface composition is consistent with the average oxidation number of chromium, as determined from chemical analysis (*1*) and redox cycles performed during the ESR experiments. In the various surface processes, double and single arrows designate reversible and irreversible transformations, respectively.

Chromium Species in the Oxidized Samples

Stage 1 refers to ZC samples as prepared, before thermal treatments. After impregnation and drying at 383 K, chemical analysis and XPS characterization show that all chromium is in the 6+ state (*1*). The formation of the supported catalyst and the nature

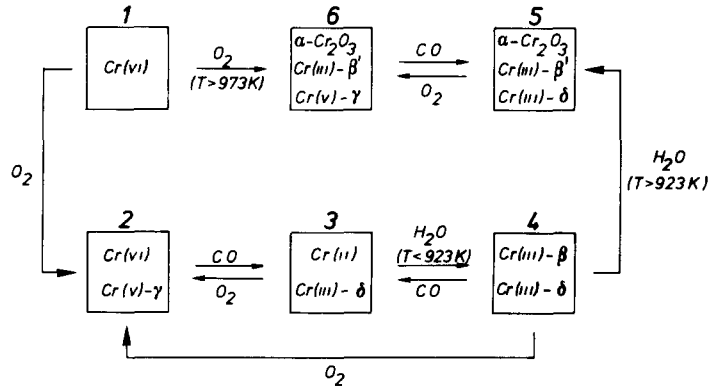

SCHEME 1. Chromium species on ZrO_2

of the interaction between surface sites of zirconia and chromium species of the CrO_3 solution are discussed in Part I and therefore are not considered here.

The s.o. treatment (1 → 2) leads to the formation of Cr(V) (γ-signal, ESR) and Cr(VI) (chromates and polychromates, IR (*3*)). As illustrated under Results, the Cr(V) fraction observed by ESR does not agree with the average oxidation number $\bar{n}$ determined by chemical means (O_2 evolution, redox cycles). The $\bar{n}$-value would suggest a Cr(V) fraction of about 50% with respect to the total Cr content. This fraction is actually the one measured on the dilute specimen ZC0.05(383)B and is closely approached by ZC0.3(383)B (Table 3), both specimens being characterized by a low Cr concentration. One is led to the conclusion that in dilute systems all Cr(V) species are seen by ESR, but as their concentration increases an increasing fraction of Cr(V) escapes ESR detection. This trend can be accounted for by the requirement that the Cr(V) species be magnetically noninteracting ("isolated"), and indeed the ^{53}Cr experiments show that only noninteracting ions are seen. While on a qualitative basis it is reasonable to expect a decrease of isolated ions as the total concentration increases, it would be desirable to obtain a quantitative ground for the observed behavior. To this end, a statistical treatment can be applied, as performed for other systems where a similar requirement for ESR detection had to be observed, such as dispersion of Ni(III) in MgO (*20*) and, closely related to the present case, Cr(V) on the surface of γ-Al_2O_3 (*9*).

In a statistical model treatment, two requisites should in principle be observed: (i) a random location of Cr(V) species over a known number of sites whose concentration is N_0 and (ii) knowledge of the minimum distance, or its equivalent in lattice spacings, necessary to render the interactions negligible and hence to allow the Cr(V) to appear as "isolated."

Some difficulties arise with respect to both points. First, not all crystallographic positions can be exchanged to adsorb Cr,

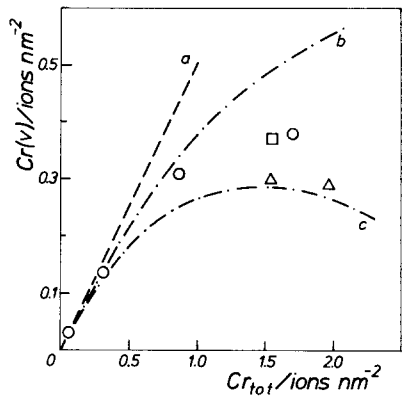

FIG. 10. *Fraction of Cr(V) detected by ESR.* A plot of the surface concentration of Cr(V) (ions nm^{-2}) vs the total Cr concentration (ions nm^{-2}) for various CrO_x/ZrO_2 samples heated in O_2 at 773 K: (○) ZCx(383), (□) ZCx(673), and (△) ZCx(923). The three curves are calculated from the equation $S = N_0 fp(1 - fp)^m$ (Eq. (1), see text). Curve (a) $f = 0.5$, $m = 0$; curve (b) $f = 0.5$, $m = 4$; curve (c) $f = 0.5$, $m = 9$.

as shown in Part I, which renders a totally random filling of sites not tenable, especially when high concentrations are reached. Second, it is difficult to assess a minimum distance for detection. However, we can apply a statistical treatment to the $Cr(V)/ZrO_2$ system with the aim of studying trends rather than absolute checks. We assume that the statistical model is obeyed, since at most 0.25 of the anionic positions are active in binding Cr-containing species. In the absence of a precise crystallographic indication, all three planes (001), (100), and (011) (Teufer's indexing (*21*)) are examined. The concentration, N_0, is taken as 7.3 ionic positions/nm^2, which is the average number of ions exposed on the three planes. The number of neighboring positions to be left empty varies between 4 or 6 (only nearest neighbors empty) to 8 or 9 (next nearest neighbors also empty), according to the plane examined (for (001), next nearest neighbors protruding above the plane are considered). We end up with two limiting values for the positions to be left empty, namely 4 to 9. The probability p that a surface site is occupied by Cr is $p = N/N_0$, where N is the concentration of Cr species (ions nm^{-2}). The proba-

bility that a site is occupied by Cr(V) is $f \times p$, where f is the fraction of Cr(V), $[Cr(V)]/[Cr_{tot}]$. In turn, the probability that Cr(V) is isolated and hence detectable by ESR is given by $fp(1 - fp)^m$, where m is the number of neighboring sites which must be empty. The concentration of isolated Cr(V) ions S is then

$$S = N_0 fp(1 - fp)^m = Nf(1 - fN/N_0)^m \quad (1)$$

The surface concentration of Cr(V) determined by ESR is reported in Fig. 10 as a function of the analytical Cr content N, for various specimens. Two curves are traced according to Eq. (1), having $f = 0.5$, as suggested before, $N_0 = 7.3$, and m equal to 4 or 9. One can see that the experimental values fall within these two curves, thereby giving weight to the model that ESR detection is limited to noninteracting species and to an approximately constant Cr(V) concentration of about 50% of total Cr present as Cr(V), in agreement with the chemical indication.

The heating with O_2 at higher temperature (above 973 K, 1 → 6) yields about the same surface concentration of Cr(V) as measured after s.o. and the segregation of chromia-like clusters (Cr(III)-β' and α-Cr_2O_3) arising from the reduction of Cr(VI) species. A different stabilization effect of the ZrO_2 matrix toward Cr(V) and Cr(VI) species is clearly identified. This aspect is discussed below.

Chromium Species in the Reduced Samples and Their Reversibility

Upon heating with CO at increasing temperature, Cr(V) is preferentially reduced in the early stages of the process, with formation of isolated Cr(III) ions not detected by ESR but identified by IR (3). After the s.r. (2 → 3), in the late stages of the reduction, Cr(VI) also is reduced to Cr(II), identified by IR (*3*), and Cr(III)-δ species are observed by ESR. The formation of Cr(III)-δ from reduction of Cr(V) possibly involves ion migration at 623 K with some clumping of Cr(III) ions. The clumping, however, is limited and does not progress to a greater extent during the subsequent heating with H_2O at $T < 923$ K (3 → 4) or higher temperature (4 → 5). By way of contrast, during the latter treatments Cr(II) is oxidized to Cr(III) with formation of chromia-like particles whose size increases with increasing temperature of heating with H_2O, in the order: β-species < β'-species ≪ α-Cr_2O_3.

On the whole two redox couples, independent of each other, are identified: Cr(V)/Cr(III) and Cr(VI)/Cr(II). Full reversibility of the couple Cr(V)/Cr(III) is maintained during the redox treatments (2 ⇄ 3, 3 ⇄ 4) even in the toughest conditions, as for instance after heating with H_2O at $T > 923$ K (5 ⇄ 6). Milder conditions ($T < 923$ K) must prevail in order to preserve the reversibility of the redox couple Cr(VI)/Cr(II), or otherwise irreversible segregation of chromia-like species occurs (1 → 6, 4 → 5).

The Stabilization Effect of the ZrO_2 Matrix

Cr(VI) and Cr(V) species, in nearly equal amounts, are stabilized on ZrO_2 after s.o. and Cr(II) and on Cr(III) after s.r. Strong interaction with the support stabilizes isolated Cr(V) ions and prevents extensive clustering of Cr(III) during the reduction process. Sites for Cr(V) on ZrO_2 must (i) allow for square pyramidal configuration, and their concentration must (ii) change in a way which is proportional to the surface area of zirconia (structure insensitive sites) and (iii) be higher on ZrO_2 as compared to SiO_2 or Al_2O_3, for which lower concentrations of Cr(V) have been reported (2% on SiO_2 and 7% on Al_2O_3, from Refs. (*9*, *7*), respectively). The last fact suggests that the chemical nature of the matrix (acid–base properties of O^{2-} and OH^- sites) plays an important role, in addition to the geometrical features of the site (point (i)).

As regards the stabilization effect on Cr(VI), the results show that these species are more loosely anchored to the surface of ZrO_2 as compared to Cr(V) species. The formation of chromia-like clusters suggests the involvement of polynuclear species of Cr(VI) as precursors and/or the higher ten-

dency of the Cr(VI) species to migrate during heating at high temperature.

The similarity of behavior of ZCx(T) samples, not only toward the adsorption of Cr but also in the stabilization of Cr species and irrespective of zirconia temperature pretreatment, has been substantially confirmed (*1*). ESR results, however, specify a somewhat higher tendency toward the segregation of clustered Cr(III) on the surface of ZCx(383) samples, as compared to both ZCx(673) and ZCx(923). The tendency is observed both toward the formation of Cr(III)-δ species during the reduction treatments and Cr_2O_3-like species during heating with O_2. Higher percentages of total Cr(III) detected as Cr(III)-δ on ZCx(383) samples (Table 3) and segregation of β'-species and α-Cr_2O_3 at lower temperatures on ZCx(383) (Table 4) are in fact observed.

ACKNOWLEDGMENT

The precious collaboration of the late Dr. S. Febbraro to the ESR analysis is acknowledged. This paper is dedicated to his memory.

REFERENCES

1. Cimino, A., Cordischi, D., De Rossi, S., Ferraris, G., Gazzoli, D., Indovina, V., Minelli, G., Occhiuzzi, M., and Valigi, M. *J. Catal.* **127,** 77 (1991).
2. Cimino, A., Cordischi, D., De Rossi, S., Ferraris, G., Gazzoli, D., Indovina, V., Minelli, G., Occhiuzzi, M., and Valigi, M., *in* "Proceedings 9th Int. Congr. Catal." (M. J. Phillips and M. Ternan, Eds.), Vol. 3, p. 1465. Chem. Inst. Canada, Ottawa (1988).
3. Cimino, A., Cordischi, D., Febbraro, S., Gazzoli, D., Indovina, V., Occhiuzzi, M., Valigi, M., Boccuzzi, F., Chiorino, A., and Ghiotti, G., *J. Mol. Catal.* **55,** 23 (1989).
4. Lindsay, P. N. T., and Peake, B. M., *J. Magn. Reson.* **47,** 365 (1982).
5. Ugliengo, P., Garrone, E., and Giamello, E., *Z. Phys. Chem. N. F.* **152,** 289 (1987).
6. Poole, C. P., "Electron Spin Resonance. A Comprehensive Treatise on Experimental Techniques," pp. 544–554. Wiley-Interscience (1967).
7. van Reijen, L. L., and Cossee, P., *Discuss. Faraday Soc.* **41,** 277 (1966).
8. Groeneveld, C., Wittgen, P. P. M. M., van Kersbergen, A. M., Mestrom, P. L. M., Nuijten, C. E., and Schuit, G. C. A., *J. Catal.* **59,** 153 (1979).
9. Poole, C. P., and Mac Iver, D. S., *Adv. Catal.* **17,** 224 (1967).
10. Percherskaya Yu, I., and Kazansky, V. B., *Kinet. Katal.* **8,** 401 (1967).
11. Derouane, E. G., Hubin, R., and Mathieu, G., *Chem. Phys. Lett.* **33,** 571 (1975).
12. Evans, J. C., Relf, C. P., Rowlands, C. C., Egerton, T. A., and Pearman, A. J., J. *Mater. Sci. Lett.* **4,** 809 (1985).
13. Spitz, R., *J. Catal.* **35,** 345 (1974).
14. Verbeek, J. L., Profschrift, Technische Hogeschool TE, Eindhoven (1968).
15. van Reijen, L. L., Thesis, University of Amsterdam (1964).
16. Shapovalova, L. A., Bryukhovetskaya, L. V., and Voevodskii, V. V., *Kinet. Katal.* **8,** 1314 (1967).
17. Fornier, J. T., Landry, R. J., and Bartram, R. H., *J. Chem. Phys.* **55,** 2522 (1971).
18. Korteweg, G. A., and van Reijen, L. L., *J. Magn. Reson.* **44,** 159 (1981).
19. Van Vleck, J. H., *Phys. Rev.* **74,** 1168 (1948).
20. Cimino, A., Gazzoli, D., Indovina, V., Inversi, M., Moretti, G., and Occhiuzzi, M., "Structure and Reactivity of Surfaces" (C. Morterra, A. Zecchina, and G. Costa, Eds.), Vol. 48, p. 279. Elsevier, Amsterdam (1989).
21. Teufer, G., *Acta Crystallogr.* **15,** 1187 (1962).